significantly lower in lung adenocarcinoma and liver cancer and higher in breast cancer, BAF155 express significantly lower in liver and kidney cancer and higher in colon, stomach, and uterine body cancer, and RBAP48 express significantly lower in liver and prostate cancer. ($p<0.01$)

Conclusions: Expression of BRM complex subunits showed negative correlation with factors indicating cancer progression in various conditions, which is consistent with reported data. The expression rate of each subunit varies by cancer types. Although BAF170 express consistently high in most of cancer types, BRM, BAF155, and RBAP48 express significantly different compare to the average.

Table 1.

	BAF170	BRM	BAF155	RBAP48
ALL	97%	27%	72%	89%
LUNG SCC	94%	31%	85%	96%
LUNG AD	99%	**5%**	59%	91%
BREAST	97%	**60%**	86%	98%
KIDNEY	98%	**13%**	**35%**	92%
BILE TRACT	96%	**10%**	62%	92%
THYROID	97%	26%	68%	82%
LIVER	92%	**4%**	**33%**	**71%**
COLON	100%	**52%**	**98%**	99%
STOMACH	100%	29%	**90%**	94%
PROSTATE	96%	43%	83%	**71%**
PANCREAS	92%	**11%**	77%	100%
BLADDER	98%	**47%**	88%	90%
OVARY	93%	23%	81%	90%
UTERINE BODY	100%	24%	**95%**	98%

1426 Loss of Histone Acetyltransferase MORF Is a Less Common, but Specific Molecular Event in Cellular Leiomyomas

Y Tang, X Zhang, HG Gao, CX Li, P Lee, JJ Wei. New York University Medical Center, New York, NY.

Background: Cellular uterine leiomyomas (C-ULM) are less common (5% of leiomyomas) and are characterized by their cellular nature. A recent study identified a new reciprocal translocation of t(10;17) from several C-ULM. The translocation disrupts the histone acetyltransferase MORF. To evaluate if loss of MORF is a common molecular event, we examined expression of MORF mRNA in large numbers of usual and cellular type ULM.

Design: Ninety cases of uterine leiomyomata were studied, of which 60 cases were of the usual type and 30 cases of the cellular type. Triplet tissue cores from usual type and cellular leiomyomata along with 2 normal matched myometrial cores were collected and arrayed in tissue microarray. The probe NYMS4 (histone acetyltransferase MORF cDNA) was prepared and cloned into TOPO vector with SP6 and T7 promoters. Digoxin-labeled probes (sense and antisense) were synthesized using SP6 and T7 DNA polymerase. In-situ hybridization was performed according to a standard protocol.

Results: MORF cRNA probe was prepared from 5' coding region. Expression of MORF mRNA was detectable with moderate intensity by in situ hybridization in both ULM and matched myometrium. In MORF mRNA positive cases, intensity of MORF mRNA was higher in ULM than that in the matched myometrium. No difference of MORF mRNA was found between usual type and cellular type. Among 60 usual type ULM, no loss of MORF mRNA was identified. However, in 3 cases out of the 30 cellular leiomyoma (10%), complete loss of MORF mRNA was present in all 3 tumor cores, but not in matched myometrium.

Conclusions: Expression of MORF mRNA is detectable in both myometrium and usual type of leiomyoma. The level of MORF mRNA expression tends to be higher in ULM. Loss of MORF is observed in 10% of C-ULM but 0% in the usual type ones. Loss of MORF is less common but specific to C-ULM, suggestive of a unique tumorigenic role of MORF in C-ULM.

1427 Expression Profiling of Colonic Epithelium by Laser Capture Microdissection Proposes a Role for Rantes (CCL-5) in the Pathophysiology of Lymphocytic Colitis

B Winn, PA Meitner, R Tavares, E Sabo, MB Resnick. Rhode Island Hospital and Brown University Medical School, Providence, RI.

Background: Lymphocytic colitis (LC) is a disorder characterized by increased numbers of T-lymphocytes infiltrating colonic epithelium. Although the histopathological features of LC are well characterized the pathophysiology of this disorder remains uncertain. Our aim was to determine whether expression profiling can identify inflammatory mediators contributing to the pathophysiology of LC.

Design: Paraffin blocks from cases of LC, collagenous colitis(CC) and aged matched controls with a history of diarrhea but histologically normal (NC) were retrieved from the pathology archive of the Rhode Island Hospital. For IHC, intraepithelial T-lymphocytes infiltrating the surface epithelium were stained with anti CD3 antibody. T-cells were enumerated microscopically and expressed as CD3 labeled T-cells per 100 epithelial cells. For laser capture microdissection (LCM) surface epithelium which included the infiltrating lymphocytes was separated from the surrounding stroma by LCM. RNA was extracted and reverse transcribed using Paradise FFPE reagents from Molecular Devices, Sunnyvale CA. The resulting cDNA was used to probe a Th1,Th2,Th3 RT^2 Profiler PCR Array (SuperArray Bioscience Corp, Frederick, MD) for the genetic expression profile of key genes involved in the inflammatory immune cascade.

Results: Six Profiler PCR arrays were run for each subgroup (6LC, 6CC, 6NC). Ten genes were upregulated 2 fold or more in the epithelium from laser-captured lymphocytic colitis as compared with normal colonic epithelium (CCL5, CCR4, GFI1, IGSF6, IRF4, JAK2, LAT, PCGF2, STAT1, TNFRSF9) whereas seven were up regulated in collagenous colitis (CCL11, CCL5, GATA3, IL5, LAT, SOCS2, TNFRSF9).

Upregulated Genes in Lymphocytic Colitis

Gene	RANTES	CCR4	GFI1	IRF4	PCGF2	STAT1	TNFRSF9
Fold Increase	12.48	4.66	2.35	2.31	2.55	2.42	2.82

Upregulated Genes in Collagenous Colitis

Gene	RANTES	CCL11	GATA3	IL5	LAT	SOCS2	TNFRSF9
Fold Increase	2.76	2.40	2.23	2.55	2.08	2.13	2.38

Conclusions: Expression profiling by LCM of archival pathology specimens is a novel technique by which to define new inflammatory mediators involved in the pathophysiology of microscopic colitis.

1428 Differential Expression of Myocyte Enhancer Factor (MEF2) Isoforms in Rabdomyosarcoma

GS Yu, T Gulick, L Balos. University at Buffalo, Buffalo, NY; Harvard Medical School, Boston, MA.

Background: Recent studies showed that MEF-2 isoforms (MEF2A, B, C and D) played different roles in muscle differentiation and neuronal maturation. MEF-2A and 2D have been shown to specifically promote differentiation and survival of cerebellar granular cells. MEF-2C-null mice are embryo lethal, while MEF-2A-null mice develop cardiac myopathy. MEF2 protein has also been detected in cardiac myxoma and rhabdomyosarcoma by using non-isoform specific MEF2 antibody. However, the expression of MEF-2 isoforms in myogenic or neurogenic tumors is unclear. This study evaluates the histologic expression pattern of MEF2 isoforms in rhabdomyosarcoma and myxoma by using immunohistochemistry with isoform-specific MEF2 antibodies.

Design: Rhabdomyosarcoma, cardiac myxoma, intramuscular myxoma, neuroblastoma and Ewing's sarcoma/PNET (primitive neuroectodermal tumor) cases were reviewed. Immunostaining with MEF2A-, MEF2C-, MEF2D-specific antibody and isoform non-specific antibody were performed with proper positive and negative controls. The stain results (intensity) were assessed by two pathologists and graded as positive (++), weak positive (+) and negative (-). The stain distribution was also evaluated as extensive (>50% of the cells) and patchy (<50% of the cells). The human left atrium is served as positive control.

Results: All the MEF2 isoform-specific and non-specific antibodies positively stained the nuclei in the control and positive cases. There is no cytoplasmic expression identified. The detailed results are listed in the table.

Conclusions: MEF2 proteins are differentially expressed in embryonal and alveolar types of rhabdomyosarcoma and cardiac myxoma but not PNET and neuroblastoma. However, only MEF2A and 2D isoforms are expressed in rhabdomyosarcoma cells while only MEF2C was expressed in myxoma cells. Our data suggests that MEF2 isoforms are differentially involved in the myogenic differentiation of rhabdomyosarcoma and cardiac myxoma, and the MEF2 antibodies may provide a new marker option in the differential diagnosis of rhabdomyosarcoma against Ewing's sarcoma and neuroblastoma.

Table. Results of Immunostains

Case	Musc. spe actin	Desmin	MEF2A	MEF2C	MEF2D	MEF2 non-spec
Rhabdo. Embryon	+	+	P++	-	P+	++
Rhabdo. Alveolar	+	+	P+	-	P+	++
Rhabdo. Botryoid	+	+	-	-	-	-
Cardiac myxoma	n	n	+	+	+	+
Intra-musc. myxoma	n	n	+	+	+	+
Ewing's/PNET	n	n	-	-	-	-
Neuroblastoma	n	n	-	-	-	-

P: patchy; N: not determined; ++:positive; +:weak positive

Pediatrics

1429 Clinicopathologic Study of the Liver of Children with Sickle Cell Disease

D Ang, PA Rodriguez Urrego, B Fyfe. UMDNJ-RWJMS, New Brunswick, NJ.

Background: Children with sickle cell (SC) anemia undergo chronic blood transfusion (CBT) therapy that may lead to liver injury. The aims of this study were to correlate histopathologic changes in liver biopsies from SC children with clinical data, laboratory values and number (no.) of transfusions.

Design: The aspartate aminotransferase (AST), alanine aminotransferase (ALT), total bilirubin (TB), serum ferritin (SF) and the no. of transfusions received up to the time of biopsy were recorded. Liver injury was assessed histologically by architectural disruption; inflammatory activity grading and fibrosis (modified Scheuer system). Pathologic grading of liver siderosis was assessed by intensity of Prussian blue staining (1-4+; 1+ is minimal focal staining, mostly Kupffer cell; 4+ is strong diffuse, definitive hepatocyte staining). TB and SF levels were correlated with no. of transfusions and severity of liver siderosis and SF were correlated using Pearson and one-tailed t-test.

Results: 18 liver biopsies from 11 patients (6 female, 5 male; 6-22 years old) were analyzed. All patients were free of viral hepatitis. The mean no. of transfusions was 42 units. AST ranged from 19-66 IU/L; ALT from 12-37 IU/L; TB from 1.1-7.9 mg/dl and SF from 717-7959 ng/ml. There was no significant correlation between TB and SF levels with increasing no. of transfusion ($R = 0.073$, p value = 0.385; $R = -0.018$, p value = 0.253 respectively). All the liver biopsies showed preserved lobular and bile duct architecture. Inflammation was present in 8 cases, 2 with grade II inflammation, 6 with grade I inflammation. 12 cases showed stage 1 fibrosis. Iron scoring was1+ (n=1), 2+ (n=7), and 3+ (n=6). There was a significant correlation between the SF level and the histopathologic grade of liver siderosis ($R = 0.598$, p-value = 0.004). Kupffer cell hyperplasia was noted in 6 (33%) cases; glycogenation of the nuclei in 7 (38.9%); extramedullary erythropoeisis in 2 (11%). Serial biopsies were available from 6 patients and showed no progression of fibrosis after a range of 11 – 71 units of transfusion.

Conclusions: Our data suggest that in pediatric SC patients, pathologic grading of liver siderosis correlated with SF levels (p value = 0.004). There was an earlier rise of TB levels than AST and ALT in CBT. There were no significant correlations between TB and SF levels with increasing no. of transfusion. Though iron stores were increased, there was little other hepatic injury in this population, even when serial biopsies were examined, none demonstrated increase in fibrosis scores.

1430 Morphoproteomic Confirmation of Constitutively Activated mTOR, ERK and NF-kappaB Pathways in High Risk Neuroblastoma with Cell Cycle and Protein Analyte Correlates: A Preliminary Study

RE Brown, D Tan, JS Taylor, M Miller, J Prichard. University of Texas-Houston Medical School, Houston, TX; Geisinger Medical Center, Danville, PA.

Background: High risk neuroblastoma (HRN) portends a worse prognosis.Because rapamycin, U0126 and bortezomib (inhibitors of the mammalian target of rapamycin [mTOR], extracellular signal-regulated kinase [ERK] and nuclear factor-kappaB [NF-kappaB] pathways, respectively) inhibit proliferation of human neuroblastoma cells; we investigated: a) the state of activation of components of the mTOR, ERK and NF-kappaB signal transduction pathways in HRN cases; and b) cell cycle and protein analyte correlates.

Design: Archival biopsy materials from three (3) patients with HRN were studied with IRB approval. Each was classified as "high risk" per the COG protocol; all were stage IV with metastatic dissemination and two had N-myc gene amplification. Immunohistochemical probes were utilized for the detection of the following antigens in these tissues: phosphorylated (p)-mTOR (Ser 2448) and one of its downstream effectors, p-p70S6K (Thr 389); p-ERK 1/ 2 (Thr 202/Tyr 204); p-NF-kappaBp65(Ser 536);Skp-2; and bcl-2. The chromogenic signal and compartmentalization (plasmalemmal,cytoplasmi c and/or nuclear) were assessed by bright-field microscopy (0-3+); the S phase-associated protein kinase (Skp-2) was quantified by an automated imaging system.

Results: Moderate to strong (2 or 3+) expressions of p-mTOR, and p-p70S6K, of p-ERK 1 / 2 and of p-NF-kappaBp65 were present. Nuclear translocation of p-p70S6K, p-ERK 1 / 2 and p-NF-kappaB, was noted. Analysis of Skp-2 revealed high percentages for nuclear expression at 45%,19% and 40%, consistent with the G1 to S phase promoting effects of convergent signaling by these pathways. There was 2+ or 3+ expression of bcl-2.

Conclusions: Morphoproteomic analysis reveals the constitutive activation of the mTOR, ERK and NF-kappaB pathways in HRN cases as evidenced by: phosphorylated mTOR,p70S6K, ERK 1 / 2 and NF-kappaBp65 protein analytes using phosphospecific probes directed against sites of activation; nuclear translocation of p-p70S6K, p-ERK 1 / 2 and p-NF-kappaBp65; and the correlative nuclear expression of Skp2 and of the anti-apoptotic protein, bcl-2. These observations appear to be the first on primary neuroblastoma specimens. Moreover, they coincide with the preclinical data and represent a starting point for studies on a larger series of cases and the design of clinical trials utilizing such small molecule inhibitors in a combinatorial strategy against HRN.

1431 Caveolin-1 and Caveolin-2 Are Expressed in Type I Pneumocytes Beginning in the Canalicular Phase of Human Fetal Lung Development

LW Browne, WE Finkbeiner, FL Baehner, RE Sobonya, KD Jones. UCSF, San Francisco, CA; AHSC, Tucson, AZ.

Background: Caveolae are invaginations on the surface of cells that serve as membrane organizing centers. Defects have been implicated in diseases of several organ systems. Three members of the caveolin family, caveolin-1 (Cav1), caveolin-2 (Cav2), and caveolin-3 (Cav3), are essential for caveolae formation. Cav1 and Cav2 are expressed in endothelial cells, adipocytes, fibroblasts, and smooth muscle cells. In human adult lung, Cav1 and Cav2 are expressed in type I pneumocytes and endothelium. Both negative and positive expression has been reported for Cav1 and Cav2 in bronchiolar epithelium. Recently, one isoform of Cav1 was identified in early fetal mouse type I pneumocytes. Since the fetal human correlate of caveolin expresssion in lung was not known, we investigated its expression by tissue microarray analysis.

Design: We built a tissue microarray with 109 1-mm cores of human fetal lung tissue, ranging in gestational age from 10-2/7 to 24 weeks as determined by fetal ultrasound. A control array of 52 1.5-mm cores of morphologically normal adult lung tissue was also built. The arrays were stained with Cav1 and Cav2, and 2+ or 3+ (scale 0-3) was considered true positive staining. The fetal lung morphology was interpreted to be in the pseudoglandular phase of development (~6-16 weeks) if airway branching was generally incomplete. The canalicular phase (~16-28 weeks) was interpreted as further airspace development with attenuated lining epithelium. Early saccular phase, which precedes actual saccular phase (~28-36 weeks), was interpreted as partial development of terminal sacs with more airway complexity.

Results: Type I pneumocytes were uniformly negative for Cav1 and Cav2 in the pseudoglandular phase, uniformly positive in the canalicular phase, and uniformly positive in the early saccular phase. Bronchiolar epithelial cells were negative for Cav1 and Cav2 in all developmental and adult stages. Normal adult endothelial and smooth muscle cells showed expected positivity for Cav1 and Cav2.

Conclusions: We report that both Cav1 and Cav2 are expressed in type I pneumocytes beginning in the canalicular phase of human fetal lung development, and we determined the lack of bronchiolar expresion of caveolin. Cav1 and Cav2 are known to be implicated in lung maturation and lung pathology, including fibrosing diseases and tumorgenesis. The canalicular phase of development could serve as a specific focus for investigations of caveolin-related mechanisms in human subjects.

1432 DAX1. A Helpful Marker in the Differential Diagnosis of Ewing Tumor

E de Alava, M Mendiola, T Hernández, J Mora, F López-Barea, I González, E Lalli, J Alonso. Centro de Investigación del Cáncer, Salamanca, Spain; IIB-H. U. La Paz, Madrid, Spain; Hospital Sant Joan de Déu, Barcelona, Spain; Hospital Niño Jesús, Madrid, Spain; CNRS, Sophia-Antipolis, France.

Background: Differential diagnosis of Ewing tumor (ET) remains a challenge. Although use of molecular genetic testing is very useful, only CD99 has been of some help in the immunohistochemical (IHC) workup of ET. CD99, however, lacks specificity in the small blue round cell tumor setting, being also expressed in small cell synovial sarcoma, some rhabdomyosarcomas, and subtypes of T-cell lymphomas. In an attempt to identify new relevant targets of EWS/FLI1 oncoprotein, a key diagnostic and pathogenetic molecule in ET, we recently demonstrated that DAX1, an orphan nuclear receptor, is a new EWS/FLI1 dependent gene, by using cDNA arrays, inducible expression of EWS/FLI1 and EWS/FLI1 silencing. In addition, we showed that DAX1 is highly expressed in a short group of ET cell lines and clinical samples (Int J Canc 2006; 118: 1381).

Design: To evaluate the interest of DAX1 expression for differential diagnosis of ET, we evaluated DAX1 expression by IHC in a series of 275 well annotated pediatric tumors, including most entities in the differential diagnosis of ET in which CD99 expression is detected. We used a monoclonal DAX1 antibody (clone 2F4, dilution 1/1000). Tumors were obtained from the National Solid Childhood Tumor Network of Spain, and 3 TMAs were performed to ensure minimal experimental variability. Two independent observers performed a semiquantitative scoring of DAX1 immunoreactivity. Only moderate-strong nuclear staining was scored as positive.

Results:

	Number of cases	Negative	Positive
Hodgkin's	28	28	0
NHL B-cell type	23	23	0
NHL T-cell type	9	9	0
Alveolar rhabdo.	21	11	10
E. rhabdo.	28	23	3
Neuroblastoma	73	65	8
Synovial	26	25	1
Ewing's	38	3	35

High DAX1 expression was frequently seen in ET (92%) and in alveolar rhabdomyosarcomas (47%), while it was very unusual in synovial sarcomas (3%) or T-cell lymphoblastic lymphomas, as shown in Table 1. *Positivity in neuroblastoma was seen in the schwannian-rich tumors, not actually in the differential diagnosis of ET. **Negative ET cases had been previously decalcified.

Conclusions: DAX1 expression is a sensitive and relatively specific marker for ET; its assessment by IHC could be of help to rule out small cell synovial sarcoma or T-cell lymphoma, two CD99-positive tumors in the differential diagnosis of ET. Supported by the Ministry of Health of Spain (FIS-FEDER G03-089, C03-10, PI052524).

1433 Angiosarcomas in Children: A Clinicopathologic Study of 15 Cases

AT Deyrup, ST Williams, DM Parham, SW Weiss, BM Shehata. Emory University, Atlanta, GA; GI Pathology, Memphis, TN; University of Arkanasas for Medical Sciences, Little Rock, AR.

Background: Angiosarcomas are extremely rare in the pediatric population and have, accordingly, been incompletely characterized.

Design: Cases coded as angiosarcoma were retrieved from institutional and consultation files. Fifteen cases were identified and reviewed for histologic features including growth pattern (vasoformative, solid), nuclear grade, mitotic rate (mitotic figures /10 high power fields), necrosis and cell morphology (spindled vs epithelioid). Clinical follow-up was obtained for all cases.

Results: Tumors predominated in females (11F:4M) and age at diagnosis ranged from birth to 21 years (mean 7.5 years). Tumors occurred in the extremities (4), mediastinum/heart (4), trunk (2), liver (2) and mouth, breast and mesentery (1 each) and ranged in size from 3.5 to 12 cm (mean 7.2 cm). All tumors showed at least focal vasoformative areas; in 11 cases, this was the predominant pattern and 2 tumors displayed extensive (> 50%) solid architecture. Epithelioid morphology was present in 6 tumors (40%); the remaining tumors displayed a predominantly spindle cell morphology. All tumors were cytologically high grade with mitotic activity ranging from 1 to 48 per 10 high power fields (mean 14). Necrosis was observed in 11 cases. Three of the patients had underlying conditions: Aicardi syndrome (1), congenital arteriovenous malformation (1) and multiple congenital hemangiomas of the liver (1). No cases were associated with Kasabach-Merritt syndrome. Clinical follow-up was obtained for all patients and ranged from 3 to 152 months (mean 35.7 months): 9 patients (60%) died of disease (3-49 months, mean 15 months), 1 patient died of iatrogenic causes and 5 patients (33%) were alive without disease (8 – 152 months, mean 75 months).

Conclusions: Pediatric angiosarcomas are aggressive tumors that appear to represent a different biologic entity from adult angiosarcomas. Unlike adult angiosarcomas, pediatric angiosarcomas predominantly involve soft tissue and parenchymal organs and are often associated with pre-existing conditions. Despite the large size of these lesions, they are not associated with Kasabach-Meritt syndrome, suggesting that tumor extent is not the primary cause of this coagulopathy.

1434 Automated EBV-Encoded RNA (EBER) In Situ Hybridization (ISH) and Immunohistochemistry Compared to Manual ISH for Detection of Epstein-Barr Virus (EBV) in Pediatric Lymphoproliferative Disorders

NK Fanaian, C Cohen, S Waldrop, J Wang, B Shehata. Emory University, Atlanta, GA.

Background: The Epstein-Barr virus (EBV), a member of the herpes family, infects the vast majority of adults, causing no known adverse medical conditions in most people. In immunocompromised patients, however, it is associated with post-transplant lymphoproliferative disorder (PTLD), AIDS-related lymphoma, the African form of Burkitt lymphoma, some cases of Hodgkin disease, and nasopharyngeal carcinoma. Detection of EBV may be achieved by various methods, including EBV-encoded RNA (EBER) in situ hybridization (ISH), and immunohistochemistry (IHC) for latent membrane protein (LMP-1). We compared automated ISH and IHC techniques in pediatric lymphoproliferative disorders, with results by manual ISH.

Design: Thirty seven pediatric cases previously studied by manual EBER ISH included 18 EBER-positive (15 PTLD, 2 lymphoproliferative disorders, 1 immunodeficiency), 15 EBER-negative (2 PTLD, 3 lymphoid hyperplasia, 4 transplanted livers, 6 transplanted hearts) and 4 EBER-equivocal (3 atypical lymphoid infiltrates, 1 transplanted liver). Using the Bond-max autostainer (Vision Biosystems), ISH and IHC were performed with prediluted EBER probe and EBV-CS 1-4 at 1:50 dilution, respectively.

Results: Twenty cases were EBER-positive by automated ISH (15 positive, 4 negative, 1 equivocal by manual ISH). These twenty EBER-positives included 13 PTLD, 4 lymphoid hyperplasia, 2 transplanted livers, and 1 immunodeficiency. Eight cases positive by IHC (7 positive, 1 negative, and none equivocal by manual ISH) were all PTLD. Compared to manual EBER ISH as gold standard, automated ISH had a sensitivity and specificity of 94% and 69% respectively, accuracy = 83%, positive predictive value (PPV) = 79%, and negative predictive value (NPV) = 90%. Automated IHC had a sensitivity = 44%, specificity = 93%, accuracy = 67%, PPV = 88%, and NPV = 59%. Automated ISH and IHC correlated significantly ($p < 0.045$).

Conclusions: Automated ISH is recommended for diagnosis of EBV-related pediatric neoplasms, being easy to perform and interpret, requiring only set-up technologist time, and with high sensitivity and NPV. The automated IHC protocol is of too low sensitivity for routine use, although results show high specificity and PPV, and correlate with automated ISH.

1435 BRD-NUT Oncoproteins: A Family of Closely Related Nuclear Proteins Associated with Aggressive Human Carcinomas

CA French, C Ramirez, AK Tadavarthy, JL Kutok, JC Aster. Brigham and Women's Hospital, Boston, MA; Harvard Medical School, Boston, MA; Allina Laboratories, St. Paul, MN.

Background: An unusual group of aggressive carcinomas are characterized by translocations that involve *NUT*, a novel gene on chromosome 15. In about 2/3rds of cases, *NUT* is fused to *BRD4* on chromosome 19. We sought to identify variant partner gene(s) of *NUT,* and to characterize the oncogenic functions of BRD-NUT proteins.

Design: *NUT*-variant carcinomas were subjected to FISH, RT-PCR, immunohistochemical, and immunoblot analysis to identify variant partner(s). GFP- and GAL4- fusion constructs were used to map nuclear export and transcriptional activation domains by fluorescence microscopy and in luciferase reporter assays, respectively. siRNA-knockdown of BRD4-NUT in BRD4-NUT carcinomas was performed to assess BRD4-NUT oncogenic function.

Results: Here, we identify the first variant fusion partner for *NUT*, *BRD3* on chromosome 9. *BRD3-NUT* and *BRD4-NUT* encode highly homologous fusion proteins composed of two tandem bromodomains, the Brd extra-terminal (ET) domain, and almost the entirety of NUT. While BRD3 and BRD4 are known to bind to acetylated histones, the function of NUT is unknown. We show here that NUT contains nuclear localization and nuclear export sequences that normally permit nuclear/cytoplasmic shuttling via a leptomycin-sensitive pathway, whereas BRD3-NUT and BRD4-NUT proteins are retained in the nucleus. NUT also contains two potent transcriptional activation domains, which are revealed when fused to the DNA-binding domain of GAL4. Unexpectedly, we observed that the knock down of BRD4-NUT with siRNA in cell lines derived from BRD4-NUT carcinomas induces squamous differentiation and cell cycle arrest.

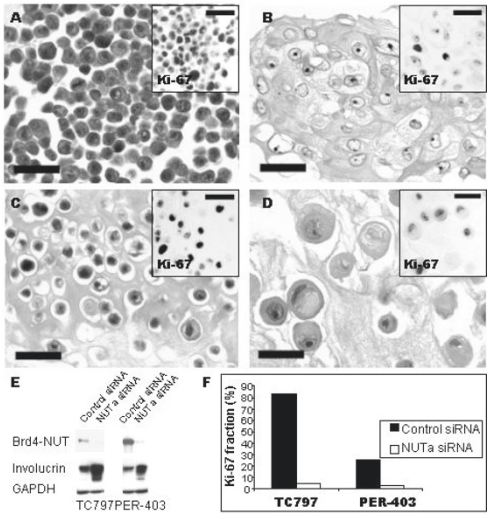

Conclusions: Altogether, these data suggest that both Brd and NUT-derived motifs likely contribute to carcinogenesis, and that Brd-NUT oncoproteins act (at least in part) through the blockade of terminal differentiation, a mechanism that has been commonly invoked in acute leukemias, but which is rare in carcinomas.

1436 Expression of XIAP Protein in Neuroblastomas and Ewing Sarcoma Family Tumors

SB Galli, M Tsokos. NCI/NIH, Bethesda, MD.

Background: XIAP (X chromosome-linked inhibitor of apoptosis protein) belongs to the family of IAPs (inhibitor of apoptosis proteins) and has been shown to inhibit apoptosis induced by various stimuli, including chemotherapeutic agents, in different cell types. The IAPs are the only known endogenous caspase inhibitors. More detailed *in vitro* studies regarding XIAP, have shown that it is the most potent inhibitor IAP family member. It inhibits not only the effector caspases 3 and 7, but also the initiator caspase 9. Expression of XIAP has been reported in several tumors, but its expression in Ewing sarcoma family tumors (ESFT) and neuroblastoma (NB) is unknown.

Design: We examined the expression of XIAP by immunoblotting in 13 ESFT cell lines (TC-32, TC-71, TC-248, TC-268, 5838, TC-300, TC-324, TC-389, TC-390, TC-392, TC-394, TC-399, TC-400) and 9 NB cell lines (CHP-126, IMR-32, SMS-SAN, SKN-AS, KCNR, SY5Y, TC-371, TC-378, TC-401). Jurkat cells were used a positive control. In 9 ESFT and one NB cell lines which have been recently established in our laboratory, we had the opportunity to study early passages and in 5 of them formalin-fixed paraffin-embedded tumor tissue was available for comparison. In addition, tumor tissue was available in 5 more earlier established cell lines (3 ESFT and 2 NB). In all these cases the tumor tissues were also evaluated for XIAP expression by immunohistochemistry (IHC). A commercially available anti-XIAP monoclonal antibody was used.

Results: All ESFT and NB cell lines showed variable expression of XIAP by immunoblotting. However, only 3 ESFT and 1 NB tissues were found positive by immunohistochemistry. We noticed that recent tumor specimens corresponding to the early passages of the recently established cell lines were more consistently positive (4 out of 5) for XIAP than older specimens (0/5). The reason for this finding is unclear at the moment.

Conclusions: Our data demonstrate that XIAP is widely expressed in NB and ESFT cells and therefore, may play a role in their response to chemotherapy. More extensive tissue studies will help address its potential implication in patient outcome.

Detection of XIAP protein by IHC in Ewing tumor (1) and Neuroblastoma (2)

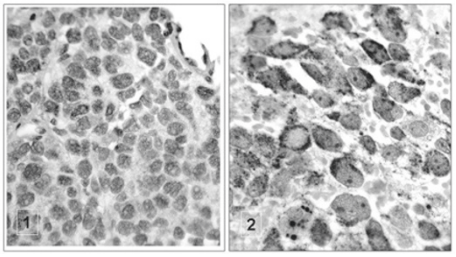

1437 Myoepithelial Carcinoma in Children

BC Gleason, CDM Fletcher. Brigham and Women's Hospital and Harvard Medical School, Boston, MA.

Background: Primary myoepithelial tumors of soft tissue are rare, and criteria for malignancy have only recently been established. Of 49 myoepithelial carcinomas of soft tissue in the literature, 9 occurred in children (of which 7 were reported by our group). We have subsequently seen 18 additional cases, and we report the clinicopathologic features of all 25 herein.

Design: 25 myoepithelial carcinomas in patients under age 18 were retrieved from the consultation files of one of the authors. For confirmation of myoepithelial differentiation, we required immunoreactivity for keratin or EMA as well as either S100, GFAP or a myogenic marker (SMA or HHF35). As previously reported, tumors were classified as malignant on the basis of moderate to severe cytologic/nuclear atypia.

Results: There were 14 females and 11 males; age at diagnosis ranged from newborn to 17 years (median 9 years). Sites included extremities (13 cases: 3 dermal, 8 subcutaneous, 2 subfascial), trunk (5 cases), viscera (5 cases: 3 mediastinal, 1 retroperitoneal, 1 intracardiac), and head/neck (2 cases). Size ranged from 1 to 11 cm. Tumors were typically heterogenous, with epithelioid, clear, spindle and/or plasmacytoid cells forming nests, trabeculae or solid sheets in a myxoid or hyalinized stroma. Epithelioid cells predominated in the majority (24 cases) and in several cases had scant cytoplasm with round cell morphology. Chondroid differentiation was present in 3 cases, metaplastic bone in 1, and ducts in 2. Mitoses ranged from <1 to 68 per 10 HPF (median 8); necrosis was present in 12 cases. Keratin was positive in all cases (CAM 5.2 in 94%, AE1/AE3 in 71%, panK in 63%), and EMA in 60%. Either S100 (72%+) or GFAP (50%+) was positive in all but 2 cases; the latter 2 had typical morphology of myoepithelial neoplasms and expressed both myogenic and epithelial markers. Clinical follow-up (range 3 months to 8.5 years; mean 1.9 years) is available in 16 cases; 1 additional patient died from post-operative complications. 8 patients (50%) had local recurrences at 1.5 months to 2.5 years after excision; 6 (38%) have developed metastases to lymph nodes, liver, lungs, bone, soft tissue, or orbit at 1.5 months to 8 years; and 5 (31%) have died of disease at 6 to 21 months (mean 12 months). All 3 patients with visceral tumors for whom clinical follow-up is available died despite aggressive chemotherapy.

Conclusions: Despite the rarity of carcinomas in the pediatric population, myoepithelial carcinoma appears to be overrepresented among children and often has an aggressive clinical course, particularly those arising at visceral sites.

1438 Outcomes Based Analysis of Criteria Proposed by the Placental Pathology Practice Guideline Development Task Force: Oregon Experience

V Kolesnikova, JM Guise, T Morgan. OHSU, Portland, OR; Oregon Health & Science University, Portland, OR.

Background: Our objective was to test whether implementing published guidelines from the Placental Pathology Practice Guideline Development Task Force regarding chorioamnionitis and funisitis improved sensitivity of detecting clinically significant patient outcomes. Specifically, we hypothesized that the presence of umbilical cord arteritis and/or chorioamnionitis not involving the amnionic epithelium (two features commonly not diagnosed by general surgical pathologists) will be associated with lower APGAR scores at 5 minutes.

Design: We performed a retrospective analysis of 100 consecutive placentas submitted to the OHSU department of pathology. Ten cases were excluded because of insufficient sampling (e.g. no umbilical cord, etc). Patient history and APGAR scores were provided by the State Obstetric and Pediatric Research Collaboration (STORC). Preterm labor was a common indication for pathology (n=49). Placental findings were compared between general surgical pathologists (OHSU faculty), a placental pathologist (T.M.), and trained pathology resident (V.K.). The presence of funisitis was qualified as the presence or absence of arteritis. Chorioamnionitis (CA) was evaluated in the fetal membranes and placental chorionic plate and staged as described (e.g. CA1 is neutrophils associated with chorion, CA2 is infiltrating chorion, CA3 is infiltrating amnionic membrane).

Results: We observed a good correlation between TM and VK (kappa statistic 0.80, 0.64 for umbilical cord and placenta, respectively) and a moderate correlation with general surgical pathologists (kappa 0.41, 0.58), who showed a relatively decreased frequency of diagnosing funisitis (7% vs 16%) and chorioamnionitis (17% vs 25%). Scoring the chorionic plate for inflammation compared to membranes showed no significant improvement in the correlation with funisitis or APGAR scores. Culture data was available for only 2 placentas and was excluded. Significant associations were identified between decreased APGAR scores and the presence of umbilical cord arteritis (Mann-Whitney U test, P-value 0.05), and increasing stage of chorioamnionitis (CA3, P<0.01; CA2, P<0.05; CA1 not significantly different than negative placentas).

Conclusions: General surgical pathologists diagnosed severe chorioamnionitis (CA3) and approximately half of the cases of funisitis, but failed to identify arteritis and chorionitis (CA2), which appear to be associated with significantly decreased APGAR scores.

1439 Immunohistochemical Evaluation of FLI-1 in Acute Lymphoblastic Lymphoma: A Potential Diagnostic Pitfall

O Lin, DA Filippa, J Teruya-Feldstein. Memorial Sloan Kettering Cancer Center, New York, NY.

Background: Acute lymphoblastic lymphoma(ALL) is a rare neoplasm that is more commonly seen in children and adolescents. Histologically, ALL is characterized by a population of small round blue cells with an open nuclear chromatin pattern. One of its main differential diagnosis is Ewings Sarcoma/Primitive Neuroectodermal Tumor (ES/PNET) an entity with which it shares some morphologic and immunohistochemical features. Both tumors are immunoreactive for CD99. Approximately 90% of ES/PNET have a specific t(11; 22)(q24;q12) that results in fusion of the EWS and FLI-1 genes, and overexpression of FLI-1 protein, which has been reported to be expressed in approximately 70% of ES/PNETand 80% of ALL,B-cell phenotype cases. Therefore, it is possible that a case of CD45 negative ALL immunoreactive for CD99 and FLI-1might lead to a misdiagnosis of ES/PNET with critical clinical and treatment management implications. The objective of this study is to evaluate a panel of antibodies that would allow a correct diagnosis of ALL and determine the frequency of FLI-1 immunoreactivity in a series of ALL cases of either T- or B-cell phenotype.

Design: The study cohort comprised ALL of either T- or B- cell phenotype consecutively ascertained at our institution between 1995 and 2005. The histological diagnosis was based on hematoxylin and eosin (H&E) staining and immunohistochemical studies. Representative TMA or whole tumor sections from formalin-fixed,paraffin embedded blocks were submitted for a panel of immunohistochemical markers including: CD3, CD20, CD43, CD45(LCA), CD99, FL1 and TdT using established Ventana protocols for the Ventana Benchmark® processor (Tucson, AZ). Tumors were scored using criteria previously published.

Results: Twenty cases of ALL were evaluated and showed the following results. Immunoreactivity for CD3 was seen in 12/20 (60%), CD20 in 5/20 (25%), CD43 in 19/20(95%), CD45 in 15/20(75%), CD99 in 15/20 (75%), FLI-1 and TDT in 17/20 (85%) cases. Two cases negative for LCA, CD20 and CD3 were positive for FLI-1, CD99, TdT and CD43. Two other LCA negative cases were positive for CD99 but negative for FLI-1. All cases showed immunoreactivity for CD43, TdT or both.

Conclusions: Immunostains for CD43, TdT or both was present in all cases of ALL and should be included in the immunohistochemical evaluation of small round blue cell tumors. Absence of immunoreactivity for LCA does not exclude ALL and immunoreactivity of FLI-1 is not restricted to ES/PNET.

1440 Proteomic Identification and In Vitro Assessment of Heat Shock Protein 90 (HSP90) as a Potential Target for Ewing Tumor Treatment

AS Martins, A García-Sánchez, D Herrero-Martín, C Mackintosh, A Otero, M Campos, T Hernández, JL Ordoñez, E de Alava. Centro de Investigación del Cáncer, Salamanca, Spain.

Background: Ewing Tumor (ET) is a malignant neoplasm characterized by having several deregulated autocrine loops that mediate cell survival and proliferation. Therefore their blockade is a promising therapeutical approach. We previously reported the in vitro impact of IGF1R/KIT pathway blockade on ET cell lines, and we now extend our observations to the level of proteomic changes induced by this treatment.

Design: 2D gels and mass spectrometry (MALDI-ToF) studies of ET cell lines treated with ADW742 (ADW) and/or Imatinib (IMA) (specific IGF1R/cKIT inhibitors) were performed and results confirmed at protein/mRNA levels. To analyze the impact and mechanism of HSP90 inhibition, one of the proteins showing high expression changes, we used one specific inhibitor, the 17-allylamino-17-demethoxygeldanamycin (17-AAG), as well as immunoprecipitation studies to assess the physical intercation of HSP90 to its client proteins.

Results: We found a large panel of differentially expressed proteins involved mainly in stress-induced responses. HSP90 was one of the proteins showing higher expression changes. Its blockage with 17-AAG was effective in inhibiting ET growth and survival, especially in cell lines that were previously resistant to IGF1R/KIT pathway blockade. We also showed, for the first time in ET, that 17-AAG treatment induced HSP90 client protein degradation, including AKT, mTOR or IGF1R, by inhibiting their physical interaction with HSP90. This is a potentially important finding, as IGF1R signaling pathway is very relevant in sarcoma pathogenesis. Combination of 17-AAG and ADW/IMA was synergistic.

Conclusions: HSP90 blockage effectively inhibited growth and survival in ET cell lines, especially in those resistant to IGF1R/KIT pathway blockade treatment. Importantly, sensitivity to drugs such as ADW/IMA depends not only on the levels of expression and basal activation of their receptors IGF1R/KIT, as previously shown, but also, and for the first time described in ET, on the quality of the stress response mechanism.

1441 Muscle Coenzyme Q10 Predicts Abnormal Mitochondrial Respiratory Chain Enzyme Activity in Children

L Miles, PH Tang, KE Bove, PS Horn, P Morehart, B Wong, T deGrauw, MV Miles. Cincinnati Children's Hospital Medical Center, Cincinnati, OH; University of Cincinnati.

Background: Mitochondrial respiratory chain enzyme (MRCE) deficiency is an important biomarker for diagnosis of mitochondriopathy in children. We reported relationships between CoQ content and mitochondrial markers in pediatric muscle biopsies (Miles et al. *Pediatr Neurol* 2005;32:318), and proposed that muscle CoQ10 may be useful for screening for mitochondriopathy in children. Here we hypothesize that low CoQ10 content in muscle is correlated with abnormal MRCE activity.

Design: This study was approved by the IRB. Muscle biopsy specimens from 77 children (<17y) were acquired between 2/2004-1/2006. A detailed description of laboratory methods is provided in the previous reference. All specimens were tested for MRCE activity by a reference laboratory. Abnormal MRCE activity was defined as ≤30% of the reference lab's mean normal values for one or more MRCE complexes. Data were dichotomized as normal (Gp 1) and abnormal (Gp 2) MRCE activity. Statistical analysis was conducted using Spearman correlation, Mann-Whitney U test, and step-wise logistic regression. A P-value <0.05 was considered significant. The unit of CoQ10 components is nmol/g protein. Results are expressed as mean±SEM.

Results: Abnormal MRCE activity was reported in 12 of 77 muscle specimens. Age, sex, and race were similar for Gps 1 and 2 (age 5.9±0.6 and 4.6±1.4y, respectively). Total, reduced, and oxidized CoQ10 were decreased in Gp 2 (total=169±20 vs 235±9, P=0.003; reduced=59±10 vs 81±4, P=0.036; oxidized=109±12 vs 155±7, P=0.005). Significant correlations were noted between total, reduced, and oxidized CoQ10 vs. each MRCE activity except complex III. Significant correlations also existed between % subsarcolemmal mitochondrial aggregates (SSMA) and complexes I+III, II+III, III, and IV; but none correlated with type 1 myofiber predominance. Logistic regression of CoQ10 components, % SSMA, and % type 1 myofibers on Gps 1 and 2 indicated that total CoQ10 was the strongest predictor of abnormal MRCE activity (P<0.0001; area-under-the-ROC curve=0.774). By optimizing for classification accuracy it was determined that a cut off value of <186 for CoQ10 provides 75% sensitivity and 83% specificity (P<0.0002; Fisher's exact test) for abnormal MRCE activity.

Conclusions: Determination of total CoQ10 content <186 in muscle is a useful test for predicting abnormal MRCE activity in children, and may assist in screening for mitochondriopathy.

1442 Massive Hepatocyte Losses in Hepatic Hemophagocytic Lymphohistiocytosis (HLH) Are Mediated by Induction of Fas/FasL (CD95/CD95L) Apoptosis Pathway and Not the Cytotoxic Cell Induced Perforin/Granzyme Pathway or the Beclin-1 Autophagy Pathway

BY Ngan, SC Ling, VL Ng, S Weitzman. Hospitial for Sick Children, U. of Toronto, Toronto, ON, Canada; Hospital for Sick Children, U. of Toronto, Toronto, ON, Canada.

Background: Massive lymphohistiocytic infiltrates in the bone marrow, lymph nodes, liver or spleen occur in both familial and non-familial Hemophagocytic Lymphohistocytosis (HLH). Some familial forms have perforin gene mutations and reduced NK/ cytotoxic cell functions. Regardless of the perforin gene mutation or abnormal NK cell functions, massive cell loss limited to the liver can occur. In this study we examined if such hepatocyte destruction was mediated by Programmed Cell Death (PCD) Type I (apoptosis via the CD95/CD95L, or the cytotoxic cell mediated perforin pathway) or PCD Type II (Beclin 1 mediated autophagy).

Design: Liver biopsies from 3 HLH patients and the liver-explant from 1 liver transplant patient (ages:7 days to 3 years) were studied. All had some clinical evidences of HLH (fever, cytopenia, hypertriglyceridemia, hypofibrinogenemia and/or hyperferritinemia) and 2 had perforin gene mutation or mild decreased NK cell function. Cytotoxic T/NK-cell and macrophages were assessed by immunohistochemistry (IHC) by using CD8, 56, 57, granzyme A, B, TiA-1, perforin, S-100, CD1a, CD163, 68, and Mac 387. Hepatocyte apoptosis was detected by IHC using antibodies to cleaved caspase3, cleaved PARP, M30, Fas(CD95)/FasL(CD95L). Mediation by the autophagy pathway was assessed by electron microscopy and IHC with antibody Beclin 1.

Results: Increases of macrophages in hepatic sinusoids with prominent hemophagocytosis, portal lymphocyte infiltrates and hepatocyte loss were found. In the 2 patients with perforin mutations, perforin containing cytotoxic cells were low, but massive hepatocyte losses persisted. Some hepatocytes were apoptosis marker^{+ve} but all were Beclin-1^{-ve}. Many infiltrating macrophages and lymphocytes were CD95L^{+ve} and the hepatocytes had membranous staining for CD95.
Conclusions: Hepatocyte losses in HLH appeared to be triggered by PCD type I through the engagement of CD95L from HLH lymphohistiocytic cells with its receptor CD95 on the hepatocyte membrane. PCD was not dependent on the functional competency or the numbers of the perforin/granzyme^{+ve} cytotoxic lymphocytes.

1443 Microstatelite Instability: Is There a Role for DNA Mismatch Repair Proteins MLH1, MSH2 and MSH6 in Wilms Tumor?

RM Przygodzki, A Plotsky, J Horn, AA Ahmed. Children's National Medical Center, Washington, DC.
Background: Nephroblastoma (Wilms tumor - WT) is the most common genitourinary cancer in children. Despite tremendous efforts in elucidating molecular markers of aggressiveness in WT, there is a lack of information whether DNA mismatch repair protein expression may play such a role.
Design: Seventeen formalin-fixed, paraffin-embedded WT displaying favorable and unfavorable (nuclear anaplasia) histologies, as well as localized, metastatic and bilateral tumors formed the basis of this study. Adequate tumor sampling and histologic studies were performed to confirm the diagnosis. Samples underwent immunostaining with antibodies to DNA mismatch repair proteins MLH1, MSH6 and MSH2 utilizing heat-epitope pretreatment. Appropriate controls were employed, as was normal embryological kidney tissue for additional comparisons. Slides were blindly reviewed identifying extent and pattern of immunostaining with each antibody and subsequently compared to stage and presence of nuclear anaplasia.
Results: Thirteen favorable histology and 4 diffuse NA WT were identified. Eight WT cases had tumor confined to the kidney or extending beyond the renal capsule (stage 1 and 2, respectively), 2 were localized to the abdomen (stage 3), 4 showed distant metastases (stage 4), and 3 showed bilateral renal tumors (stage 5). Immunostaining revealed a propensity for diffuse nuclear staining among stage 1 and 2 WT whereas patchy negatively staining clusters of blastemal tumor cells dominated the remaining tumor stages (MLH1 $p<0.01$, MSH2 $p<0.003$, MSH6 $p<0.01$). All WT with nuclear anaplasia displayed similar patchy negatively staining blastema, with nuclear anaplastic cells usually showing total lack of staining or less commonly rare individual cell staining with all antibodies. Bilateral WT displayed similar patchy negatively stained nests of blastema. In all cases, the epithelial cells, when present, were reactive with the antibodies. In comparison, embryonal kidney revealed positive nephrogenic zone comma and S-body staining with all three antibodies, and positive staining of nephrogenic zone blastema with MLH1 and MSH2.
Conclusions: WT with aggressive characteristics, i.e., having nuclear anaplasia or presenting with bilateral renal tumors, displayed patchy negatively staining clusters of blastema with MLH1, MSH2 and MSH6 antibodies. These findings suggest clonal blastema expansion wherein DNA mismatch repair protein expression is lacking, which may further lead to genetic instability, and increased tumor aggressiveness.

1444 Chordomas in Children and Young Adults: Clinical and Histopathologic Features

RV Ridenour III, CY Inwards, DV Miller. Mayo Clinic, Rochester, MN.
Background: Recent reports suggest that younger patients with chordoma may represent a unique subset of patients with differing clinical aggressiveness and treatment responsiveness compared to older adults. We report a series of younger patients with chordoma from our institution.
Design: Chordoma patients in the Mayo Clinic files from 1910 to 2006 were identified. The age distribution was graphed and an appropriate younger-aged study population selected. Tumor location, surgical procedures, adjuvant therapy and outcome were assessed by retrospective chart review. H-E stained sections were reviewed with systematic scoring of histologic subtype, necrosis, mitoses and cytologic atypia.
Results: A total of 460 cases of chordoma were identified in patients ranging from ages 8 to 85 (mean 51). Forty-seven patients less than 25 years old (mean age: 18) formed the first peak of a bimodal age distribution pattern and were selected for study. 23 were male and 24 female. Chordomas of the spheno-occipital (SO), mobile spine (MS), and sacrococcygeal (SC) region comprised 74%, 15%, and 11% respectively in this group (compared to 34%, 17%, and 49% for those over age 25). Conventional (42%) and chondroid (29%) chordomas were the most frequent subtypes in younger patients and were associated with survival rates of 84% and 100% respectively. Young patients with cellular (11%), poorly differentiated (16%), and dedifferentiated (2%) chordomas had less favorable survival, 40%, 29%, and 0% respectively. Necrosis, mitoses, and cytologic atypia were highest and most frequent in these more aggressive subtypes. Young patients with SC chordoma had worse survival and were more likely to be of the cellular or poorly differentiated subtypes. Chordomas located in the SO region showed better survival and were more likely to be of the conventional or chondroid subtype (except for a sole case of dedifferentiated chordoma). Chordomas of the MS showed survival and histologic subtypes intermediate between those of the SC and SO regions. 85% of patients received radiation therapy, which was associated with better survival versus surgery alone (77% v. 40%).
Conclusions: In this series, chordomas in patients younger than age 25 demonstrate substantial biologic differences in terms of histologic subtype, location, and behavior when compared to tumors in older adults. They also represent a distinct peak of a bimodal age distribution curve seen for all patients with chordoma.

1445 CD61 Expression on Rhabdomyosarcomas: A Curious and Cautionary Tale

MR Roullet, M Paessler, JK Choi. Hospital of the University of Pennsylvania, Philadelphia, PA; Children's Hospital of Philadelphia, Philadelphia, PA.
Background: Rhabdomyosarcoma (RMS) can present as a bone marrow (BM) tumor without obvious soft tissue mass and can morphologically mimic acute myeloid leukemia (AML). RMS can be distinguished from AML by immunophenotyping for muscle markers but these markers are not typically examined in a standard flow cytometry analysis for AML. In this study, we report the flow cytometry findings of RMS.
Design: Cases of RMS from 2002-5 were reviewed retrospectively and 5 cases were identified that were also analyzed by flow cytometry for possible leukemia or lymphoma. These cases were also analyzed by routine histology, paraffin immunohistochemistry (PIHC) for myogenin, von Willebrand Factor & CD61, cytogenetics, and molecular studies for the PAX3- or PAX7-FKHR fusion transcripts.
Results: Metastasis to the BM (3 cases) and lymph node (1 case) were seen in 4 patients. The last patient had RMS restricted to a single soft tissue mass. The diagnosis of RMS was confirmed by PIHC for myogenin that showed strong nuclear staining. Flow cytometry of all 5 tumors showed a distinct population that was CD45 negative with low to moderate side scatter. Dim CD61 reactivity was seen in the 4 metastatic RMS but not in the 1 non-metastatic RMS. PIHC for von Willebrand Factor and CD61 was negative, suggesting that the dim CD61 reactivity is non-specific or below the sensitivity of PIHC. Molecular and cytogenetic studies were available on 3 patients, all with metastatic RMS. Within these 3 patients, 2 had PAX3/7-FKHR fusion transcripts. One case was notable for the RMS restriction to the BM and its morphologic and immunophenotypic similarities to AML-M7. The aspirate smears revealed a discohesive large mononuclear tumor cells with round to irregular nuclei, fine chromatin, indistinct nucleoli, and scant to moderate cytoplasm. Cytochemistry performed on the aspirate smears showed MPO-, SBB-, NSE-, and block PAS positive tumor cells. Flow cytometry demonstrated CD45-, CD61+, and CD34+ tumor cells. Only the focal spindle morphology of the tumor cells on the BM biopsy raised the suspicion of RMS that was confirmed by PIHC and cytogenetics.
Conclusions: On flow cytometry, RMS are CD45- with low side scatter and can show CD61, CD34, and CD7 reactivities, mimicking AML-M7. The immunophenotype and morphologic features of AML do not exclude a diagnosis of RMS. CD61 expression appears to correlate with metastasis and may be a potential marker for RMS with a predilection for wide spread metastasis.

1446 Desmin Immunopositivity Differentiates Lipoblastoma from Other Lipomatous Tumors

AG Saad, T Archibald, JD Goldsmith, H Kozakewich, L Debelenko. Children's Hospital, Boston, MA; Beth Israel-Deaconess Medical Center, Boston, MA.
Background: Lipoblastoma is a benign pediatric tumor that can be difficult to differentiate from other lipomatous lesions. Cytogenetics is helpful in the definitive diagnosis of lipoblastoma but is often not available and identification of immunohistochemical markers would be beneficial. Desmin immunopositivity noted by us in an immunohistochemical panel for a recently encountered lipoblastoma prompted this study.
Design: We performed desmin immunohistochemistry (mouse monoclonal antibody, Biogenex) on formalin-fixed paraffin-embedded sections of 39 lipomatous lesions (34 children, 5 adults) including lipoblastoma (n=9), lipoma (n=5), lipofibroma (n=4), fibrous hamartoma (n=11), myxoid liposarcoma (n=4) and atypical lipomatous tumor/well differentiated liposarcoma (ATL/WDLS, n=6) retrieved from our pathology files during the past 15 years. Only lipoblastomas and lipomas with known diagnostic cytogenetic abnormalities (aberrations of long arms of chromosomes 8 and 12, respectively) were selected for the study. Appropriate positive and negative controls were applied throughout.
Results: All 9 cytogenetically confirmed lipoblastomas showed strong desmin expression in spindled cells within fibrous septa and lobules. Immunopositivity was extensive in the immature lesions and was moderate and mainly restricted to fibrous septa in the mature (lipoma-like) forms. One of 4 myxoid liposarcomas had rare desmin-positive cells within spindle-cell fascicles and one of 6 ATL/WDLSs showed rare desmin-positive spindled cells in the fibrous septa. All cytogenetically confirmed lipomas as well as lipofibromas and fibrous hamartomas were immunonegative.
Conclusions: Desmin immunopositivity of lipoblastoma is a useful feature and helps to differentiate it from mimics such as myxoid liposarcoma and lipoma. Lipoblastoma should now be considered in the differential diagnosis of desmin-positive tumors in children, which can help avoid diagnostic pitfalls in small biopsies. We hypothesize that desmin-positive spindled cells in lipoblastoma may be pluripotent mesenchymal cell derivatives in a transient state of myogenous differentiation.

1447 Increased Expression of Fatty Acid Synthase in Pediatric High-Grade Lymphomas

AC Seegmiller, J Willis, S Kamrudin, D Rakheja. UT Southwestern Medical Center, Dallas, TX; Children's Medical Center, Dallas, TX.
Background: Fatty acid synthase (FASE) catalyzes the synthesis of fatty acids from acetyl CoA. It is highly expressed in metabolic organs, but at very low levels in most other tissues. Recent studies have demonstrated increased expression of FASE in a variety of tumors. Furthermore, high FASE levels are often associated with more aggressive behavior and worsened prognosis, and inhibitors of FASE activity have been shown to decrease proliferation and increase apoptosis of tumor cells. Very little is known about FASE expression in hematolymphoid malignancies. This study evaluated the expression of FASE in pediatric high-grade lymphomas, compared to reactive lymph nodes.

Design: An institutional database was searched for pediatric cases of high-grade lymphoma, including diffuse large B-cell lymphoma (DLBCL), Burkitt lymphoma (BL), anaplastic large cell lymphoma (ALCL), lymphoblastic lymphoma (LL), and reactive lymph nodes. FASE expression was evaluated by immunohistochemistry using anti-FASE mouse monoclonal IgG (IBL Co., Japan). Normal skin, which contains both FASE-positive and negative cells, was used as a control. Expression was quantified as the average of two scores: (1) 0-3 score for intensity of staining, and (2) 0-3 for proportion of cells stained. Two pathologists scored each specimen independently. In cases of disagreement, the specimens were rescored jointly to achieve consensus.
Results: Database searches yielded 38 cases (7 DLBCL, 7 BL, 6 ALCL, 8 LL, 10 reactive) of adequate size and quality for evaluation. The reactive cases expressed FASE at low levels (average expression score = 0.9±0.2). FASE expression was significantly higher in DLBCL (2.4±0.2; p<0.001), ALCL (2.6±0.2; p<0.001), and LL (2.0±0.3; p=0.02). In contrast, FASE expression in BL was very low (0.7±0.3).
Conclusions: These results indicate that the expression of FASE is upregulated in DLBCL, ALCL, and LL, but not in BL, relative to benign reactive lymph nodes. This pattern of expression indicates that FASE is not simply a marker of proliferation, since the most proliferative tumors (BL) did not show significant FASE expression. Further studies are required to determine whether this is an independent marker of prognosis. However, it does raise the possibility that FASE could be studied as a specific therapeutic target in these diseases.

1448 Maternal Obesity Affects Placental Weights

L Swanson, C Bewtra. Creighton University Medical Center, Omaha, NE.
Background: Recent studies have shown increase in weights of the normal placentas. Some studies have indicated maternal obesity as a causative factor. We attempt to verify these findings.
Design: All normal, live, singleton, near term (35-42 weeks gestation) placentas delivered in the years 1995 and 2004 are compared for maternal BMI (body mass index), age, race, parity, gestational age, and weights of the babies and the placentas. All cases of maternal diabetes, hypertension, placental infection and fetal anomalies are excluded. All placentas are weighed and examined microscopically in standardized manner. 2-tailed chi square test is applied for statistical comparisons.
Results: In all, 200 cases met all criteria (118 in 1995; 82 in 2004). There is a significant increase in the maternal mean BMI from year 1995 to 2004 (25.1 vs. 26.5; p=0.024). This parallels a similar increase in the mean placental weights (499 gms vs. 537; p=0.008). The increase in BMI also correlates with the increases in the weights of the baby (p=0.001) and the placentas (p=0.001). Unlike previous reports, the maternal weight gained during the pregnancy appears unchanged over the years and does not show any correlation with the initial BMI or the baby and placental weights. Maternal race, age and parity do not show any associations with BMI or placental weights.
Conclusions: There has been a significant rise in the maternal BMI and the weights of the baby and the placenta. The actual weight gained during the pregnancy shows no significant changes. Increases in maternal and baby weights are associated with various pregnancy complications. In view of the rising trend of obesity in general population, these findings may be of clinical significance and need to be validated in larger populations.

1449 E2F3 Overexpression in Wilms Tumors

M Tretiakova, EJ Kort, KA Furge, JD Chen, L Farber, A Cornelius, XJ Yang, BT Teh. University of Chicago, Chicago, IL; Van Andel Research Institute, Grand Rapids, MI; DeVos Children's Hospital, Grand Rapids, MI; Northwestern University, Chicago, IL.
Background: The E2F3 transcription factor has an established role in controlling cell cycle progression, and has a potential role in predicting tumor aggressiveness. In our recent molecular study the E2F3 gene was found to be uniquely upregulated in Wilms tumors (WT), but not in other renal neoplasms. The goal of this study was to validate the E2F3 gene expression by immunohistochemistry (IHC) in WT tissue microarray (TMA), and to define prognostic parameters specific to E2F3.
Design: Affymetrix gene expression analysis was performed on 23 WT and compared to normal renal tissue. E2F3 activation was validated through drug treatment assay in vitro using flavinoid Silibinin, natural inhibitor of E2F3 levels in cells. IHC staining was performed in TMA with 40 WT (26 primary, 14 metastatic) and 12 normal kidneys, and correlated with Ki67 proliferation marker. Nuclear expression of E2F3 and Ki67 was quantified by using Automated Cellular Imaging System (Clarient).
Results: Elevation of E2F3 gene levels was found in all WT cases as compared to normal kidney counterparts. WT cases with stages 3 and 4, and cases who died of disease, had significantly higher expression of the E2F3 gene (Kolmogorov-Smirnov rank test p-value=0.01). We found that cases with the lowest E2F3 gene expression tended to have a longer 5-year progression free survival (p=0.06). Treatment with Silibinin induced apoptosis in WT cells, but not in control cells from clear cell renal carcinoma (% caspase positive cells by flow cytometry after 48 hours of Silibinin exposure, p<0.05). By IHC analysis, E2F3 nuclear expression was identified in all WT (3.6-85.1% positive cells) whereas the normal kidney showed no nuclear positivity. Nuclear ratios were significantly higher in metastatic tumors (p<0.05), and strongly positively correlated with proliferation rates (r=0.77).
Conclusions: Both the E2F3 gene and protein are overexpressed in WT, in contrast to the normal kidney. E2F3 levels directly correlate with tumor aggressiveness, and may have prognostic value. Selective toxicity of Silibinin to WT derived cells may predict tumor responsiveness to targeted therapy.

1450 Glypican 3: A Novel Diagnostic Marker for Pediatric Gonadal and Extragonadal Germ Cell Tumors

DL Zynger, ND Dimov, C Luan, PM Chou, XJ Yang. Northwestern University, Chicago, IL; Children's Memorial Hospital, Chicago, IL.
Background: Glypican 3 (GPC3) is a heparin sulfate surface molecule that participates in cell signaling, functions in embryonic cell differentiation and has been recently described as an oncofetal protein. A previous report of adult testicular germ cell tumors revealed that GPC3 was over-expressed in yolk sac tumor compared to other germ cell tumor histologic subtypes. The purpose of this study was to evaluate the expression of GPC3 in pediatric germ cell tumors and determine the utility of GPC3 as a diagnostic marker in this population.
Design: Sections from paraffin embedded blocks from 56 cases of pediatric germ cell tumors, including 29 gonadal (16 testicular, 13 ovarian) and 22 extra-gonadal (6 intracranial, 5 sacrococcygeal, 4 retroperitoneal, 3 mediastinal, 4 other) primary tumors and 5 lymph node metastases, were subjected to immunohistochemistry with a monoclonal antibody specific to GPC3. Histologic components were analyzed independently (30 yolk sac tumors, 29 teratomas with mature elements, 8 teratomas with immature elements, 3 germinomas, 2 embryonal carcinomas, 1 choriocarcinoma). Immunoreactivity was semi-quantitatively assessed for percent of cells stained (0, <5%; 1+, 5-10%; 2+, 11-50%; 3+, >50%) and intensity (0-3).
Results: All yolk sac tumor components had cytoplasmic and membranous GPC3 immunoreactivity (3+, 83%; 2+, 13%; 1+, 3%) with a mean staining intensity of 2.9. Expression was consistent in all growth patterns observed (endodermal sinus, microcystic, macrocystic, solid, and micropapillary). In contrast, all teratomas with mature elements were negative. Some immature teratomatous elements showed weak, variable immunoreactivity (2+, 25%; 1+, 13%; 0, 63%) and had a mean intensity of 0.9. All cases of germinoma and embryonal carcinoma were negative. The single case of choriocarcinoma was diffusely positive (3+, 100%).
Conclusions: GPC3 is expressed in yolk sac tumor, choriocarcinoma and some immature teratomatous components, but is not observed in teratoma with mature elements, embryonal carcinoma and germinoma. These results demonstrate that GPC3 is a novel diagnostic marker for primary and metastatic gonadal and extragonadal pediatric germ cell tumors, particularly yolk sac tumor. GPC3 immunohistochemistry may be useful as yolk sac tumor can be difficult to identify because it develops in many different locations, displays various histological patterns, and can form small foci that become obscured by a background of mature teratomatous elements.

1451 GPC3 Immunohistochemical Expression in Fetal and Adult Tissues

DL Zynger, ND Dimov, LJ Eisengart, C Luan, XJ Yang. Northwestern University, Chicago, IL.
Background: Glypican 3 (GPC3) is a heparin sulfate surface molecule that acts during development. Patients with GPC3 mutations have an increased risk of embryonal malignancies. The role of GPC3 in tumor biology is controversial as is theorized to be an oncofetal protein in liver, and a tumor suppressor gene in lung, ovary, and breast. However, most prior studies utilized cell culture or molecular modalities. We investigated the immunohistochemical expression of GPC3 in normal fetal and adult tissue to help elucidate its function and to more precisely define aberrant expression.
Design: Paraffin-embedded sections from 49 types of normal fetal and adult tissues were subjected to immunohistochemistry using a monoclonal antibody to GPC3. Cytoplasmic and membranous immunoreactivity was semi-quantitatively evaluated as negative (<5% cells stained), weak positive (5-10%), positive (11-50%), or strong positive (>50%). Fetal tissue (n=98) included products of conception (n=94) as well as autopsy cases (n=4) and ranged from 9 to 39 weeks gestational age. Adult tissue (n=215) was obtained from routine surgical (n=206) and autopsy cases (n=9) and ranged in age from 25 to 91 years.
Results: All placenta, fetal liver, and fetal kidney expressed GPC3. Staining was seen in syncytiotrophoblasts, cytotrophoblasts, fetal hepatocytes, developing glomeruli, and occasional developing renal tubules. Three-fourths of adult kidney expressed weak GPC3, only in renal tubules, and no adult liver demonstrated reactivity. Most fetal lung had staining in the primitive alveoli, mesenchyme, and bronchial epithelium. Interestingly, adult lung, ovary and breast were negative, as were the fetal counterparts. No expression was seen in other fetal tissues. A minority of adult tissues had weak or patchy GPC3 staining (stomach, pancreas, endometrium, adrenal) and all others were negative.
Conclusions: All fetal liver, lung, kidney and placenta express GPC3 whereas immunoreactivity in the adult is predominately limited to the kidney. This expression pattern does not support its role as a tumor suppressor but instead strengthens the theory that GPC3 is an oncofetal protein. As well, defining the normal expression of GPC3 is important to assist in the interpretation of staining when used as a diagnostic marker.

	Placenta	Liver	Kidney	Lung	Testes	Ovary	Breast
Fetal	100% (8/8)	100% (9/9)	100% (6/6)	89% (8/9)	60% (6/10)	0% (0/1)	0% (0/1)
Adult	n/a	0% (0/35)	75% (3/4)	0% (0/9)	0% (0/63)	0% (0/9)	0% (0/4)